Three-Dimensional Velocity Obstacle Method for UAV Deconflicting Maneuvers

Yazdi I. Jenie* Erik-Jan van Kampen† Coen C. de Visser‡ Joost Ellerbroek§ Jacco M. Hoekstra¶

Control and Simulation Section, Faculty of Aerospace Engineering, Delft University of Technology

Autonomous systems are required in order to enable UAVs to conduct self-separation and collision avoidance, especially for flights within the civil airspace system. A method called the Velocity Obstacle Method can provide the necessary situational awareness for UAVs in a dynamic environment, and can help to generate a deconflicting maneuver. This paper focuses on the assessment of the Velocity Obstacle Method application and its ability to resolve various conflict situations in three dimensional space. This assessment results in a redefinition of the criteria of avoidance. A novel technique is introduced to support the avoidance decision, by representing the conflict situation in various avoidance-planes. Several new definitions to support the method are introduced. This method is then implemented in three-dimensional simulations for UAVs in cases of conflict, in which more than one option of resolution is provided.

Nomenclature

ϕ	Dihedral angle of the avoidance-plane from the XY-plane, [-]
θ_{az}	Azimuth angle of the Velocity Obstacle Cone, [-]
θ_{az}	Elevation angle of the Velocity Obstacle Cone, [-]
θ_{P_ϕ}	Dihedral angle between B_{vo} and P_ϕ, [m]
θ_{vo}	Opening angle of the Velocity Obstacle Cone, [m]
A_{vo}	Apex of the Velocity Obstacle Cone, [m]
B_{cc}	Collision Cone base-circle, [-]
B_{vo}	Base-circle of the Velocity Obstacle Cone, [m]
C_{vo}	Center of the base of the Velocity Obstacle Cone, [m]
CC	Collision cone set of obstacle, [m/s]
d_{avo}	Distance of avoidance starting point from the obstacle, [m]
D_{oi}	Vector line from the ownship A_o to obstacle, [m]
d_{oi}	Distance of the own-ship from the obstacle, [m]
d_{vo}	Length of the axis of symmetry of Velocity Obstacle Cone, [m]
DIV	Diverging Zone set, {[m/s] ; [m/s]}
G_{vo}	Generating line of the Velocity Obstacle Cone, [m]
H_{vo}	Axis of symmetry of the Velocity Obstacle Cone, [m]
l_{vd}	VO-DIV intersection line, {[m] ; [m]; [m]}
P_ϕ	Avoidance Plane at the angle ϕ, [-]
r_{vo}	Radius of the base-circle of Velocity Obstacle Cone, [m]
RV	Reachable Velocity set, {[m/s] ; [m/s]}
S_{pz}	Protected Zone, {[m] ; [m]}
S_{VO_P}	Area of the Velocity Obstacle on the respective P_ϕ, [m^2]
V_o, V_i	Velocity of A_o, Velocity of A_i,[m]

*PhD Student, Faculty of Aerospace Engineering, Delft University of Technology, 2629HS, Delft, The Netherlands

†Assistant Professor, Faculty of Aerospace Engineering, Delft University of Technology, 2629HS, Delft, The Netherlands

‡Assistant Professor, Faculty of Aerospace Engineering, Delft University of Technology, 2629HS, Delft, The Netherlands

§Assistant Professor, Faculty of Aerospace Engineering, Delft University of Technology, 2629HS, Delft, The Netherlands

¶Professor, Faculty of Aerospace Engineering, Delft University of Technology, 2629HS, Delft, The Netherlands

V_R Relative velocity between two vehicles [m/s]
V_{avo} Avoidance velocity, $[m/s]$
$V_{avo}^{\min}$ Closest point for avoidance velocity, $[m/s]$
VO Velocity Obstacle set, {[m/s] ; [m/s]}
X_o, X_i Position of the own-ship, Position of the obstacle, [m]

I. Introduction

With its rapid technology advancement, UAVs are getting their civilian-commercial values recognized. It is predicted that UAVs will soon 'blacken the sky', integrate with the civil airspace system, and create a whole new type of traffic. Ref 1 gives several predictions on the usage of UAVs for civilians purposes. Once this integration is allowed, the expansion of UAVs into the airspace is inevitable; Many manufacturers and operators will race to exploit them, such that managing their air traffic will be a major concern. Since the UAVs will range widely in type and mission, dependence on a common ground station and predefined airways, like in manned-flight, is impractical. Ref.2 suggests the use of the self separation (or free flight) concept[3,4] that allows free routing and optimization of each vehicle separately.

The self-separation concept switches the task for separation keeping as well as collision avoidance to each UAV, instead of a ground control station. This task, however, will be difficult to be handle manually, due to the operators lack of situational awareness. The task is suggested to be handled autonomously.[5] Hence, research for UAVs is currently focused more on an autonomous Conflict Detection and Resolution (CD&R) system. Ref.2 presents a method for such a system that generates a deconflict maneuver[5,2] that is guided by common rules of the air. The method is called the Selective Velocity Obstacle (SVO) Method and it is an extension of the Velocity Obstacle Method (VO-method). The SVO method is able to generate an avoidance path for each UAV separately and to resolve every conflict that occurs, despite being heterogeneous.

Those demonstrations however, are restricted to a two-dimensional scenario, where it is assumed that the UAVs fly at the same altitude. This makes the SVO inadequate for UAVs that can use the full three dimensional space. In fact, the VO-method itself has been developed mainly in two dimensions since the first works on it are for land-robots. Currently there are only a few publications that mention application of the VO-method on three dimensional cases. Among them are the works of Ref.6,7, that uses the VO-method to support conflict visualization for a pilot in a non autonomous manned-flight.

This paper focuses on the assessment of the Velocity Obstacle method in three dimensional cases of UAV conflicts, and on how a resolution strategy can be decided upon. The VO-method is explained in a similar manner as Ref.2, elaborated by its criteria, algorithm, and strategy. The main goal is to modify the former VO-method for the three dimensional space, especially for UAVs applications. The modification is focused on the three main VO-method sets, i.e. the Velocity Obstacle, VO, the Diverging Zone, DIV, and the Reachable Velocity, RV. A novel technique is introduced that represents the conflict situation in various avoidance-planes. These avoidance-planes will help the autonomous system to decide which avoidance is the fastest, or which has the least risk. The avoidance maneuver will consider the deconflicting maneuver, in which the avoidance is conducted with as small of a deviation from the original path as possible. Since it is still preliminary, any uncertainties in the flight data are neglected.

This paper is structured as follows. After this introduction, the second section discusses the concept of the original Velocity Obstacle Method for deconflicting maneuver, as the basis of this research. This is the VO-method for two dimensional encounter cases. Section III explains the VO-method set definitions in three-dimensional space. The concept of avoidance-plane is introduced specifically in the following Section IV along with several new deifnition and calculation techniques to help the decision making for avoidance. Section V presents the implementation of the three-dimensional VO-method in simulations. Here, several encounter cases, as well as choice of avoidance are simulated and discussed. Section VI ends the paper with several concluding remarks.

II. Velocity Obstacle Method

This section explains briefly the Velocity Obstacle method[8,9,10,11,12,13,6,7,14,2] commonly used in the two dimensional conflict scenario between two vehicles. The explanation will take the same approach that Ref.2 used, which uses a division into the parts: VO-method criteria, algorithm, and strategy. The objective of the VO-method in this paper is to generate a deconflicting maneuver that can avoid the protected-zone,

which, in two-dimensions, is the circle S_{pz}, as shown in Figure 1.

A. Criteria

Consider an encounter of two UAVs, the own-ship and the obstacle, flying on the same altitude, shown in a top-down point of view in Figure 1.

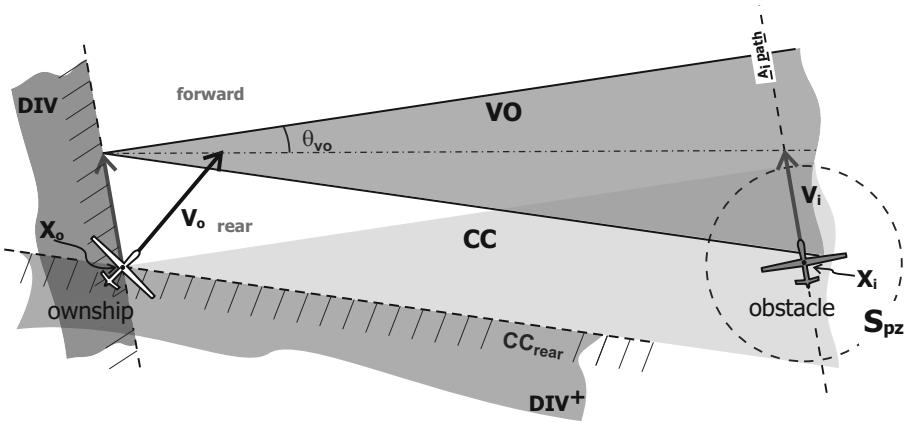

Figure 1. Two-dimensional Velocity Obstacle method. Definitions of the Collision Cone CC, the Velocity Obstacle set VO, and the new definition of the DIV set

The circle around the obstacle is the protected-zone circle, S_{pz}, that should not be violated by the ownship; violation would mean that the ownship and the obstacle collide. Both vehicles are moving with a constant velocity V_o and V_i, respectively, in a horizontal plane. With this setup, the collision cone CC can be defined as the set that collects all relative velocities V_R whose extension would intersect the S_{pz} circle. This means that CC is the area within two tangent lines of S_{pz} from the point X_o, the current position of the ownship. Hence, every combination of velocity V_o and V_i that produces a relative velocity V_R that is included in the collision cone CC will make the two vehicles collide, sometime in the future.

The velocity obstacle set, VO, is produced by translating the CC along the obstacle's velocity V_i. The VO-method also defines a diverging set, DIV, in which every V_o that is diverging from the obstacle's flight path is collected. The DIV is defined as one of the half-planes separated by the V_i line that does not contain the VO set. This definition, however, is found inadequate since it does not consider the part of the obstacle's flight path that has been passed. Ref.14 noted several cases of late restoring in the avoidance, since even after the obstacle is cleared, the ownship has to stay in maintain mode until it crosses the flight path. This paper introduce a new definition of the diverging set DIV as a collection of velocities that diverge from the obstacle A_i and its path ahead, excluding the part of the path that is already passed. The rear edge of CC is the direct connection for this, producing a DIV as a summation of the half-plane by V_i (the original definition of DIV) and the CC rear area (the DIV^+), as shown in Figure 1.

The VO-method uses the sets to describe an encounter situation in the VO criteria as follows:

C_1^{vo}: An encounter between the ownship and an obstacle-i is imminent if, and only if, $d_{oi} \leq d_{avo}$.

C_2^{vo}: The ownship will violate the S_{pz} of an obstacle-i sometime in the future if, and only if, $V_o \in VO_{oi}$.

C_3^{vo}: The ownship is diverging an obstacle-i if, and only if, $V_o \in DIV_{oi}$.

The first criterion, C_1^{vo}, is an additional criteria to decide whether the encounter between two vehicles is imminent or not, based on the distance between them, d_{oi}, and the choice of distance to start avoidance d_{avo}. The SVO presented in Ref.2 presents five additional criteria to further determine the type of encounter, and assigns right-of-way along with it. These additional criteria, however, are not discussed in this paper.

B. Algorithm

In this paper, the VO-method uses three modes: avoid, maintain, and restore. This approach is similar with Ref.[14] with a change in the first mode; the avoid-mode is used to generalize the turn-mode used for avoidance. These three modes are used especially to generate a deconflicting maneuver, a maneuver that can resolve conflict while keeping the deviation as small as possible.[5,14,2] The maintain-mode is especially defined to eliminate the oscillation problem that occurs in the basic VO-method.[15]

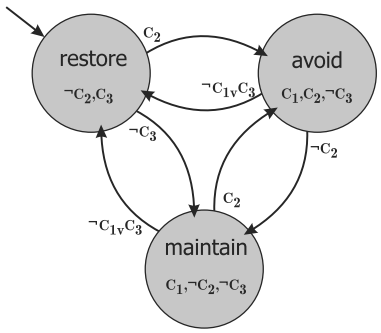

Figure 2. State transition diagram of the Velocity Obstacle method algorithm

The algorithm, shown in figure 2, works as follows: When an ownship, A_o, encounters an obstacle, A_i, the autonomous CD&R system analyzes the situation by the evaluation of the criteria. If the encounter is not imminent, or if V_o, the velocity of A_o, is diverging from the obstacle flight path, $\neg C_1^{vo} \vee C_3^{vo}$, then A_o can continue its original mission, or from the VO point of view, stay in its restore-mode. If the encounter is imminent and A_o is not diverging, $C_1^{vo} \wedge \neg C_3^{vo}$, then the system needs to analyze the inclusion of V_o inside the VO. If V_o is included in vo, C_2^{vo}, then A_o should change to avoid-mode, if not, $\neg C_2^{vo}$, A_o has to change to maintain-mode. The combination of the algorithm and the VO-method criteria result in a precise and deterministic action for a vehicle to either avoid, maintain, or restore its velocity, in a dynamic encounter. The decision can be made in an instance, without requiring any prediction of obstacle movement.

C. Strategy

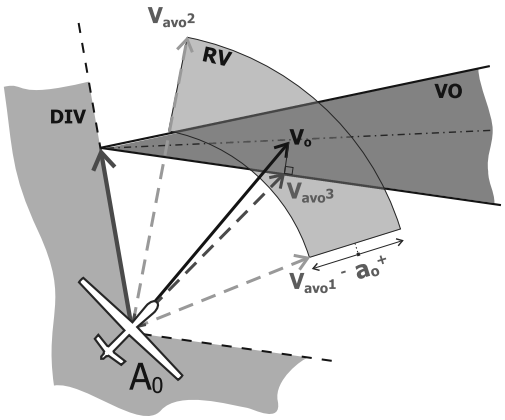

Figure 3. The Reachable Velocity Set that contains every velocity A_o can choose in its avoidance within a time-step, e.g. V_{avo^1}, V_{avo^2}, and V_{avo^3}

The strategy of the VO-method describes the option of changing velocity, within a mode selected by the UAV. The maintain-mode certainly only has one option, to keep the current velocity. In restore-mode the control of the own-ship is given back to the original control system to continue its mission. Commonly in many research of the VO-method, the restore-mode points the vehicle back to its original goal point, which is also done in this paper. Unlike the maintain and restore modes, the strategy in the avoid-mode has several variations throughout VO-research.

The strategy in the avoid-mode can be described using the reachable velocity set, RV, a collection of avoidance velocities, V_{avo} an own-ship can choose within a time-step. Ref.[14] limits the avoidance maneuver into turning only, to make it more suitable in airborne vehicle application, and thus describes the RV as an arc. Relaxing this limitation, the research in this paper will use an fan-shaped RV instead, which is still dominated by the turning maneuver, but has options to slow down or speed up, as shown in Figure 3. The strategy for avoidance is to choose the closest new velocity within the RV set, that is not intersecting with the VO. In Figure 3, the closest new velocity for avoidance is shown by the velocity V_{avo^3}, which is simply the intersection point of a line from V_o, perpendicular with VO's rear edge.

III. Three Dimensional Velocity Obstacle

The previous section presented the conventional use of the velocity obstacle in two-dimensional space, divided into three parts, the criteria, algorithm, and strategy. These three parts remain the same in three-dimensional space. The sets used, however, are redefined. They include the Velocity Obstacle set, VO, the Diverging zone set, DIV, and the Reachable Velocity set, RV.

A. Velocity Obstacle Set in Three Dimension

The work of Ref.6 and Ref.7 are two examples that extend the use of VO in three dimensions. Those works use a disk, or cylinder, to define the protected zone. The collision cone, and hence the VO, is shaped by taking the outer most lines that connect X_o with the disk. The disk shape is chosen since the work of Ref.6 and Ref.7 is used for separation assurance, with distances more than 50 NM. Vertical separation is considering the predefined traffic. Manned-flights in those distances are usually mostly horizontal. On the other hand, the three-dimensional VO-method in this paper aims to provide a method of collision avoidance for UAVs, that are expected to fill the sky with various mission and types. The flight path of each UAV is assumed to go in every direction. Therefore, this paper takes a different approach and uses a sphere, S_{pz}, to define the protected zone in space, as shown in Figure 4.

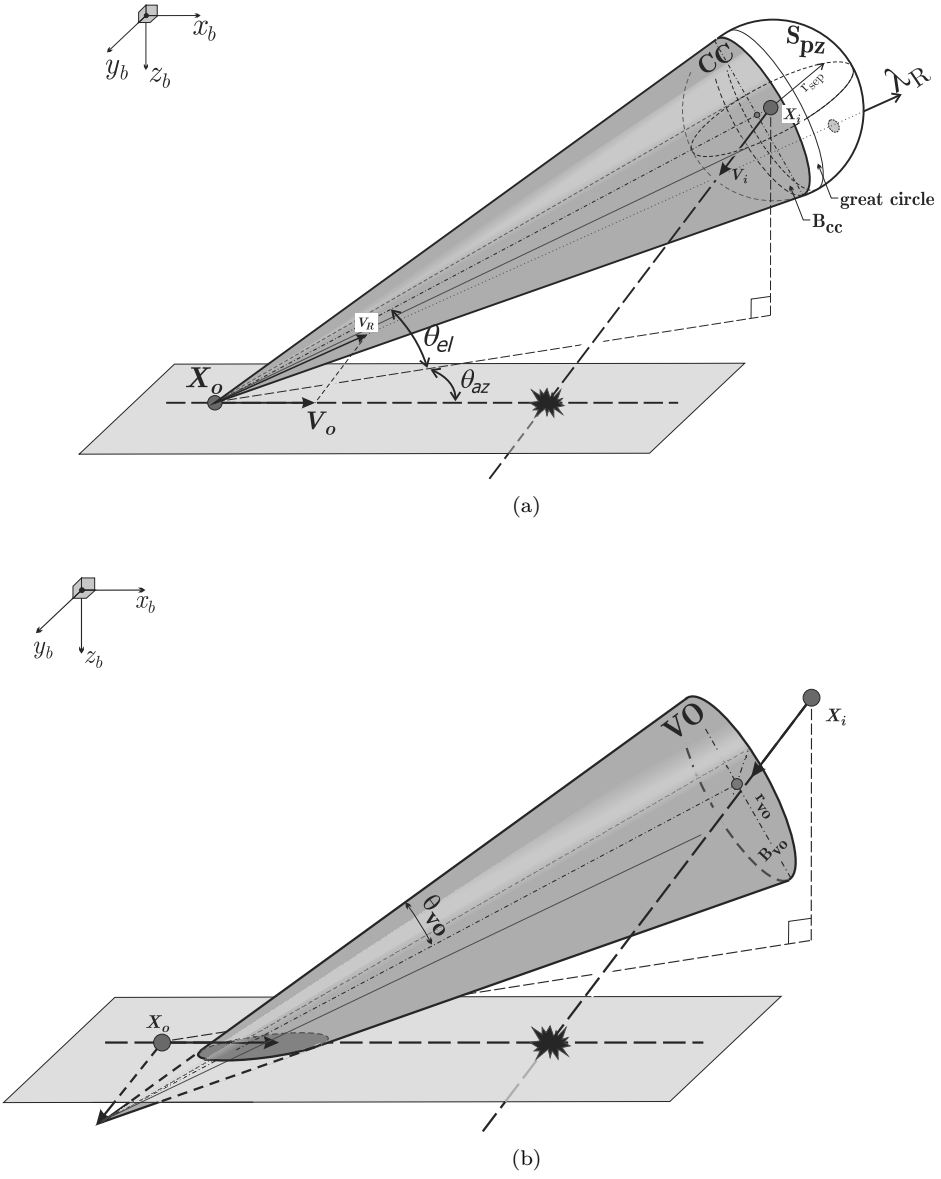

Figure 4. Three dimensional velocity obstacle set definition. (a) the Collision Cone CC, (b) Translated CC cone to the Velocity Obstacle set VO

Figure 4-a shows the collision cone, CC, as a real right-cone with as generating lines the tangent lines of the S_{pz} sphere from the point X_o. It can be observed that the CC cone is a collection of every relative velocity V_R in three-dimensions, that can extend through the S_{pz} sphere, shown for example as the λ_R line

in figure 4-a. With D_{oi} defined as the vector connecting X_o and X_i, let B_{cc} be the area perpendicular with D_{oi} as the base of CC. Notice that B_{cc} does not cut through S_{pz} on its center. In fact, since it contains all the tangent points of S_{pz} from X_o, B_{cc} will always be smaller than then S_{pz} circle.

Similar to the two-dimensional case, the VO is obtained by translating the CC along V_i, as shown in Figure 4-b. The base circle of the VO cone is defined as B_{vo}, with radius of r_vo and distance from VO apex as d_{vo}, presented in equation (1) and equation (2), respectively. The VO cone opening angle also describes the shape of the cone, and is given in equation (3)

$$r_{vo} = r_{pz} \frac{\sqrt{d_{oi}^2 - r_{pz}^2}}{d_{oi}} \tag{1}$$

$$d_{vo} = \frac{d_{oi}^2 - r_{pz}^2}{d_{oi}} \tag{2}$$

$$\theta_{vo} = \arctan \frac{r_{vo}}{d_{vo}} \tag{3}$$

In this setup, the two vehicles will collide some time in the future if $V_o \in VO$, assuming both velocities are constant. Ref.2 uses the edges of VO to determine whether V_o is included within. One alternative to determine whether the V_o point is inside the three dimensional cone VO is by transforming the V_o point to the cone's frame of reference, where the apex is the origin, and the axis is the x-axis, positive to the cone base B_{vo}, as presented in equation (4).

$$\begin{bmatrix} V'_{ox} \\ V'_{oy} \\ V'_{oz} \end{bmatrix} = \begin{bmatrix} \cos\theta_{az}\cos\theta_{el} & \sin\theta_{az} & \cos\theta_{az}\sin\theta_{el} \\ -\sin\theta_{az}\cos\theta_{el} & \cos\theta_{az} & -\sin\theta_{az}\sin\theta_{el} \\ -\sin\theta_{el} & 0 & \cos\theta_{el} \end{bmatrix} \begin{bmatrix} V_{ox} - V_{ix} \\ V_{oy} - V_{iy} \\ V_{oz} - V_{iz} \end{bmatrix} \tag{4}$$

Then, the condition $V_o \in VO$ is met if, and only if, equation (5) is fulfilled.

$$V'_{ox} > 0 \quad \wedge \quad \frac{\sqrt{{V'_{oy}}^2 + {V'_{oz}}^2}}{V'_{ox}} < \frac{r_{vo}}{d_{vo}} \tag{5}$$

B. Diverging Velocity Set in Three Dimension

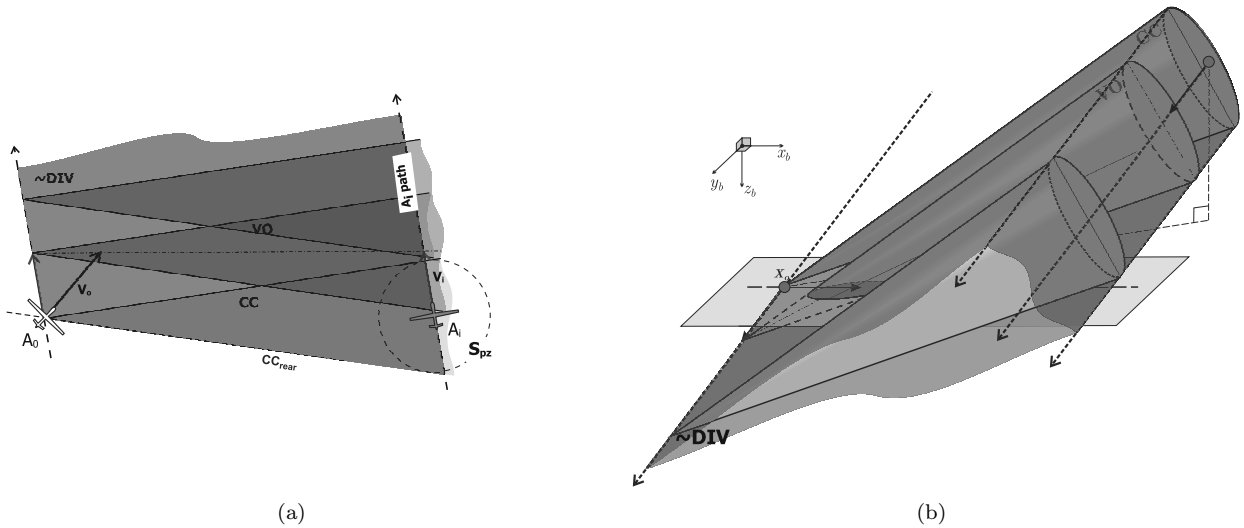

(a) (b)

Figure 5. The non-diverging set, $\neg DIV$, generation by sweeping the plane/space with the collision cone along the V_i, starting from the current A_o position. This is in order to indirectly define the Diverging Zone DIV (a) in two-dimensions; (b) In three-dimensions

The definition of diverging area in three dimensions, the diverging zone, is not as straightforward as the VO. This zone is needed to define where the A_o can safely change to the restore-mode. The diverging zone DIV can be viewed as a collection of velocities V_o that make A_o diverge from the obstacle and its path ahead. Figure 5-a shows an area in a two-dimensional situation that is generated by sweeping the Collision Cone CC, from X_o, along the obstacle velocity, V_i. The area that is not include is therefore the diverging area, DIV, as defined in the previous section. Using a similar approach, Figure 5-b shows the generation of the zone of not-diverging, $\neg DIV$, by sweeping the three dimensional space with the collision cone from the X_o along V_i. The whole space that is outside this prism-zone is therefore the diverging zone, DIV.

With this definition, the three-dimensional DIV seems to dominate the space, suggesting that the risk of conflict in three-dimensional space is much less than in the two-dimensional plane. It can also be observed that there exist parts of the VO cone that touch directly with the diverging zone. These parts are the two opposite generating-lines of the VO cone. These two lines are denoted in this paper as l_{vd}. Avoiding the obstacle by turning to the direction of one of the l_{vd} will mean that A_o is escaping as quick as possible to safety. However, because of the direct contact between VO and DIV, A_o will not experience the maintain-mode, and goes directly to the restore after escaping VO, which indicates the oscillation problem of the VO-method[15] will occur . The avoidance maneuver due to this feature needs to be further investigated by simulations.

C. The Reachable Velocity Set

In three dimensional space, a UAV can virtually turn in any direction to avoid. In accordance to the fan shaped RV in the two dimensional definition, the RV in three dimensions should be the surface revolution by the X-axis of A_o, such as shown in Figure 6. This spherical-shell shape, however, is using the assumption that there is no gravity effect that makes the shape unsymmetrical.

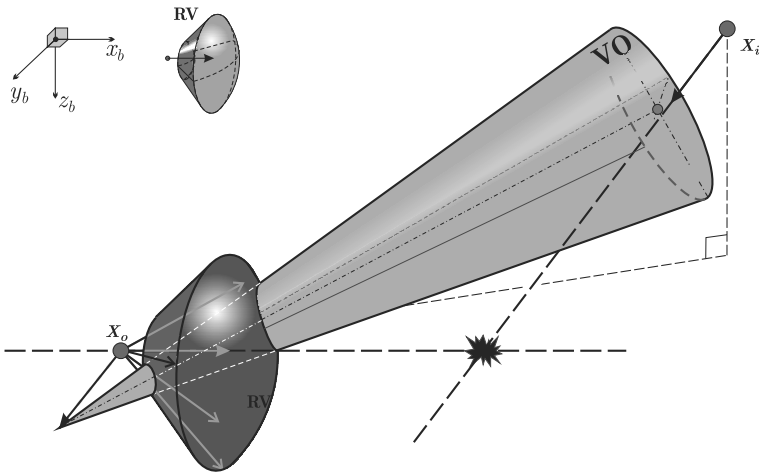

Figure 6. Reachable Velocity set, RV, definition in Three-dimensional space. The volume shape of RV is the result of surface-revolution of the two-dimensional fan-shape RV, along the X-axis.

If the strategy of avoidance remains the same, then the UAV needs to find the closest intersection point of the spherical shell RV with the VO cone. This model, however, is difficult to make sense of. This paper takes a simpler approach to assess and represent the interaction between the VO set and the RV set, by defining the avoidance planes, explained in the next section.

IV. The Avoidance Planes

The direct three-dimensional setup for the Velocity Obstacle method, explained in the previous section, is complex and thus eliminates the purpose of the method to aid in the situational awareness. Finding a good strategy hence becomes difficult. For instance, if the ownship has a reachable velocity set like the case in figure 6, then the intersection derivation from two volumes is required, i.e., between the set of RV and the VO-cone. Defining the diverging set, the RV set, and all the important intersection between them, are also difficult to illustrate. Therefore, this research introduces the avoidance planes, P_ϕ, as tools to logically

describe the three-dimensional case into separate two-dimensional setups, and provides a way to generate an avoidance strategy. This section will explain thoroughly their derivation and important parameters it has.

The avoidance plane is defined as any plane in which lies A_o's position, X_o, and velocity V_o. A UAV can therefore choose one of the planes in which it conducts the avoidance maneuver. Every set in the three dimensional Velocity Obstacle Method can be viewed as their cross-section area in each plane. By comparing between the avoidance planes, the own-ship A_o can choose the best avoidance plane and make an optimal avoidance.

Ref 7 presents a similar method of three-dimensional case breakdown, but concentrated for two avoidance planes, which are the lateral plane (XY-Plane) and the longitudinal plane (XZ-Plane).[7] The method of torus[16] for avoidance also resembles the method with an extensive calculation.

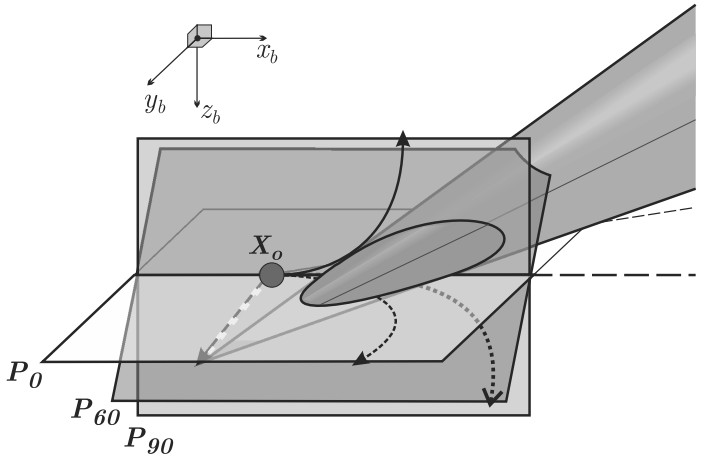

Figure 7. The avoidance plane. A_o can choose its avoidance maneuver by moving in one selected plane, e.g. P_0, P_{60}, or P_{90}.

Consider a simple case of a three dimensional encounter as shown in Figure 8. The figure shows the structure of the velocity obstacle cone in three dimensional space, for the case where A_o's position and velocity are $[0 \quad 0 \quad 0]^T$ meters and $[5 \quad 0 \quad 0]^T$ meters/second, with an obstacle encountering from the left-upper side, whose global positions are $[150 \quad 50 \quad 50\sqrt{2}]^T$ meters, heading at the global direction of $[0 \quad -45 \quad 135]^T$ degrees.

Figure 8 also shows the VO-cone as it is going through the XY and XZ -plane of the A_o body frame of reference. The cross section on the plane is an ellipse for both P_0 and P_{90}. In fact, since the VO is a right cone, for all avoidance plane, the VO cross section will be a conic-section, i.e., circle, ellipse, parabola, or hyperbola. The two-dimensional triangular shape of VO set is actually a special case of conic-section, that occurs when the VO cone apex, or the obstacle velocity V_i lies on the avoidance plane. There exist only one avoidance plane that reduce the three-dimensional case into the two-dimensional. In the next subsections, the definition of the VO, DIV and the RV, and in an avoidance plane P_ϕ is elaborated.

A. Velocity Obstacle Set on an Avoidance Plane

In order to describe the conic-section in every avoidance plane P_ϕ, the VO cone is first described mathematically in the three-dimensional space by its apex A_{vo}, its right-base circle perimeter, B_{vo}, and the center of the base, C_{vo}. These parameters are expressed using parametric equations in Euclidean space, as presented in equation (6) until (9). The derivation is conducted with the definition of the position of the own-ship according to the spherical coordinates based on the own-ship body axis as the frame of reference, XYZ_b, as shown in Figure 4-a.

$$A_{vo} = \begin{bmatrix} x_A \\ y_A \\ z_A \end{bmatrix} = V_i \tag{6}$$

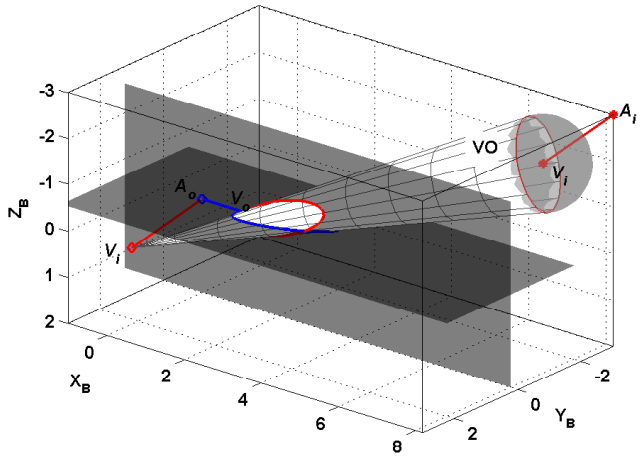

Figure 8. Example case of a three-dimensional encounter. The Velocity cone is shown, with apex on the V_i vector, crossing through the XY and XZ -plane of A_o body frame of reference.

$$B_{vo} = \begin{bmatrix} x_B \\ y_B \\ z_B \end{bmatrix} = R_{\theta_{el}|\theta_{az}} \begin{bmatrix} d_{vo} \\ r_{vo}\cos t \\ r_{vo}\sin t \end{bmatrix} + V_i, \qquad 0 \le t \le 2\pi \tag{7}$$

$$C_{vo} = \begin{bmatrix} x_C \\ y_C \\ z_C \end{bmatrix} = R_{\theta_{el}|\theta_{az}} \begin{bmatrix} d_{vo} \\ 0 \\ 0 \end{bmatrix} + V_i, \tag{8}$$

where,

$$R_{\theta_{el}|\theta_{az}} = \begin{bmatrix} \cos\theta_{az}\cos\theta_{el} & \sin\theta_{az} & -\cos\theta_{az}\sin\theta_{el} \\ -\sin\theta_{az}\cos\theta_{el} & \cos\theta_{az} & \sin\theta_{az}\sin\theta_{el} \\ \sin\theta_{el} & 0 & \cos\theta_{el} \end{bmatrix} \tag{9}$$

Every generating-line, or generatrix, of the VO cone that connects the cone apex with the base circle are expressed in equation (10). the VO cone symmetric, on the other hand, is expressed in equation (11).

$$G_{vo} = \begin{bmatrix} x_g(t) \\ y_g(t) \\ z_g(t) \end{bmatrix} = (B_{vo} - V_i)\, t_g + V_i, \qquad 0 \le t_g \le 1 \tag{10}$$

$$H_{vo} = \begin{bmatrix} x_h \\ y_h \\ z_h \end{bmatrix} = (C_{vo} - V_i)\, t_h + V_i, \qquad 0 \le t_h \le 1 \tag{11}$$

Using equation (10), the conic-section on the xy-body axis, or P_0, in particular, can be derived by assigning $z_g = 0$. The parametric t_g value in equation (10) thus can be derived, and the conic-section for P_0 can be expressed as in equation (12).

$$VO_{P_0} = \begin{bmatrix} x_{vo} \\ y_{vo} \end{bmatrix}_{P_0} = \begin{bmatrix} -(x_B - x_A)\frac{z_A}{(z_B - z_A)} + x_A \\ -(y_B - y_A)\frac{z_A}{(z_B - z_A)} + y_A \end{bmatrix} \tag{12}$$

The equation for the VO conic-section in any arbitrary avoidance plane P can be found by virtually rotating the cone around the X-axis of A_o, and use equation (10) and (12) again. The virtual rotation of thw VO cone, corresponds with the avoidance plane of P_{ϕ_p}, expressed in equation (13).

$$A_{vo}^{\phi} = \begin{bmatrix} x_A^{\phi} \\ y_A^{\phi} \\ z_A^{\phi} \end{bmatrix} = R_{P_\phi} A_{vo}, \qquad B_{vo}^{\phi}(t) = \begin{bmatrix} x_B^{\phi}(t) \\ y_B^{\phi}(t) \\ z_B^{\phi}(t) \end{bmatrix} = R_{P_\phi} B_{vo}(t) \tag{13}$$

where,

$$R_{P_\phi} = \begin{bmatrix} 1 & 0 & 0 \\ 0 & \cos\phi & \sin\phi \\ 0 & -\sin\phi & \cos\phi \end{bmatrix} \tag{14}$$

Now equation (12) can be rewritten for any avoidance plane P_ϕ as expressed in equation (15).

$$VO_{P_\phi} = \begin{bmatrix} x_{vo}(t) \\ y_{vo}(t) \end{bmatrix}_{P_\phi} = \begin{bmatrix} -\left(x_B^{\phi}(t) - x_A^{\phi}\right) \frac{z_A^{\phi}}{\left(z_B^{\phi}(t) - z_A^{\phi}\right)} + x_A^{\phi} \\ -\left(y_B^{\phi}(t) - y_A^{\phi}\right) \frac{z_A^{\phi}}{\left(z_B^{\phi}(t) - z_A^{\phi}\right)} + y_A^{\phi} \end{bmatrix}, \tag{15}$$

where

$$z_B^{\phi} \neq z_A^{\phi}, \qquad 0 \leq t \leq 2\pi \tag{16}$$

The point where the cone symmetry axis intersect with P_ϕ, can be derived in the same manner, which result in equation (17).

$$H_{P_\phi} = \begin{bmatrix} x_h \\ y_h \end{bmatrix}_{P_\phi} = \begin{bmatrix} -\left(x_C^{\phi} - x_A^{\phi}\right) \frac{z_A^{\phi}}{\left(z_C^{\phi} - z_A^{\phi}\right)} + x_A^{\phi} \\ -\left(y_C^{\phi} - y_A^{\phi}\right) \frac{z_A^{\phi}}{\left(z_C^{\phi} - z_A^{\phi}\right)} + y_A^{\phi} \end{bmatrix}, \tag{17}$$

Figure 9 shows twelve examples of conic sections of the VO cone generated in the example of Figure 8, illustrated at A_o's body axis as the frame of reference. The conic-sections of VO are shown by the shaded elliptical areas. The thick line on the x-axes represents V_o, while the thick gray line represents the projection of V_i on each avoidance plane P_{phi}. The star inside each area represent the intersection point of the symmetry axis, the $C_{vo}\phi$. The dashed line represents the projection of VO cone axis of symmetry. Due to the cone symmetry, this line will always coincides with the major axis of every VO conic-section.

Equation (15) works well in defining an ellipse area. For parabolic and hyperbolic area, however, another consideration is required. In both case, not all generating line in the finite cone of VO_P will intersect with the avoidance plane P_ϕ. This is the singular condition from the equation, when $z_B^{\phi}(t) = z_A^{\phi}(t)$. To avoid the problem, the VO_P is determined as a polygon that connects the points resulting from equation (15), only when $0 \leq t_g \leq 1$. In other words, only consider the finite VO cone. With this setup, the area on the 'other cone' in the hyperbolic result is also removed as well.

A special degenerate case is shown in P_{45}, in which V_i, or A_{vo}^{ϕ} is included in the avoidance plane. In this condition, the conic section taking a triangular shape, where all generating line from A_{vo} to B_{vo} crosses the avoidance plane P in the same point, i.e., the V_i, except for two line. The VO_P triangle area is limited by this two line, expanding until the d_{vo}. Hence, generating the VO_P using the parametric equation (15) is impossible without defining these two line. The point of these line on the base circle B_{vo}^{ϕ} can be derived using the singular condition of equation (15), that is, when $z_B^{\phi}(t) = z_A^{\phi}(t) = 0$.

The case of triangular shape is one from three degenerate cases that can occur when the cone apex, A_{vo}, is included in the P_ϕ. If the condition of $z_B^{\phi}(t) = z_A^{\phi}(t) = 0$ only result in one point on the cone base, the VO_P will be a single line. If instead there are no solution found, then VO_P will be a single point, that is the cone apex, A_{vo} itself. It is interesting to observe that on every case of encounter there always exist at least one avoidance plane P_ϕ that creates this degenerate case. If the vector of V_o is parallel with V_i, then every case of VO_P is degenerate.

In general, using the acute dihedral angle between the avoidance plane, P_ϕ and the cone base-circle B_{vo}, the type of shape of the VO_P can be defined. This angle is denoted as θ_{P_ϕ} and derived in the following equation (18).

$$\theta_{P_\phi} = \arccos\left(\frac{z_C^{\phi} - z_A^{\phi}}{d_{vo}}\right) \tag{18}$$

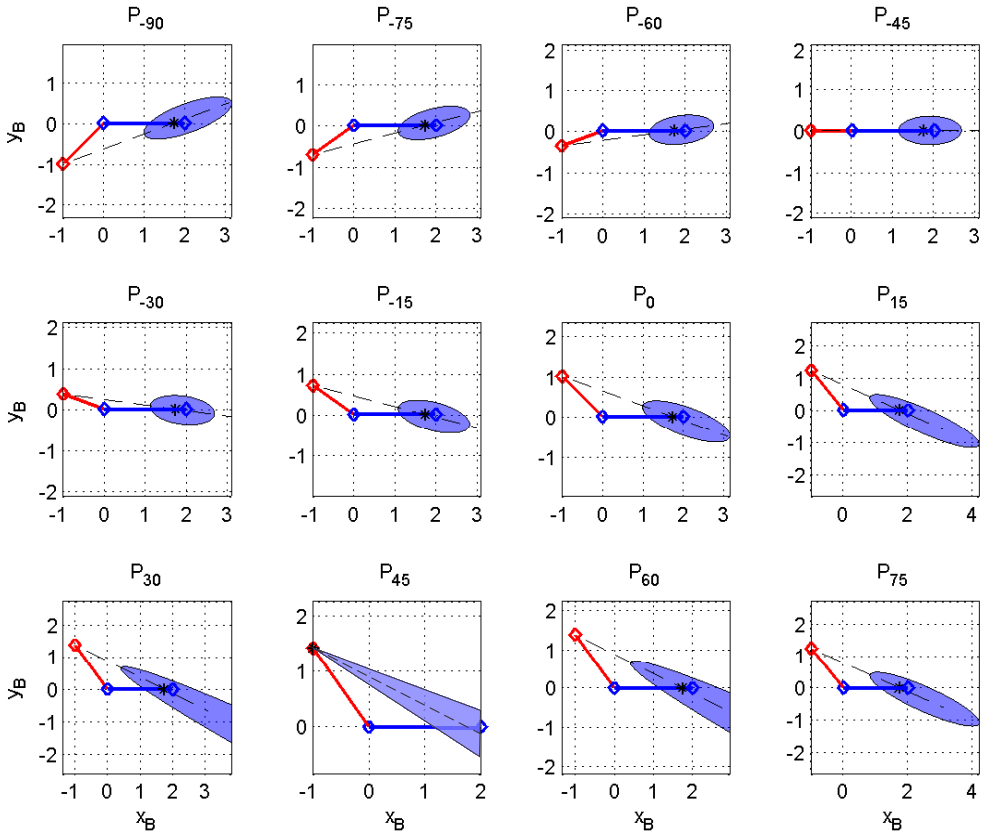

Figure 9. Conic-sections of the VO cone on several avoidance-planes. The thick blue line on X-Axis represent V_o, while the thick gray line is the V_i projection on the avoidance plane. The dashed line from V_i is the projection of VO's cone axis of symmetry.

Together with the degenerate cases, the types of area of the VO_P are summarized in the following list.

1. if $\theta_{P_\phi} = 0$, then VO_P is **a circle**, if also $A_{vo} \in P_\phi$, then VO_P is a **single point**.
2. if $\theta_{P_\phi} < \pi/2 - \theta_{vo}$, then VO_P is **an ellipse**, if also $A_{vo} \in P_\phi$, then VO_P is **a single point**.
3. if $\theta_{P_\phi} = \pi/2 - \theta_{vo}$, then VO_P is **a parabolic area**, if also $A_{vo} \in P_\phi$, then VO_P is **a straight line**.
4. if $\theta_{P_\phi} > \pi/2 - \theta_{vo}$ and P_ϕ does not cut through the VO-cone axes, then VO_P is **a hyperbolic area**, if also $A_{vo} \in P_\phi$, then VO_P is **a triangle**.

Equation (15) can be used to further determine the property of the VO_{P_ϕ} set, treating the set as a polygon. For the Velocity Obstacle Method, the most important property is whether the V_o is included in the VO_P set or not. Equation (4) still hold in this context. Another way can also be used to keep the focus on an avoidance plane, that is, by finding the intersection of the VO_P with the x-axis. If there are two intersection point, in which only one of them has value less then V_o, then the V_o is inside the VO_P.

Two other important properties are the set area, S_{VO_P}, and the closest point of V_{avo}. The area is related to the risk the ownship must consider in its avoidance on the chosen avoidance-plane P_ϕ. The smaller the area is, the more option of V_{avo} the ownship has. Figure 9 shows that P_{-45} has the smallest area, while P_{45}, as a triangle, has the largest. The closest point for avoidance, V_{avo}, however, is not only depends on the area, but on the type of shape and the area axis attitude as well. The area for a polygon with n-vertices can be defined using equation (19). The closest vertex of the polygon from the current velocity, on the other hand, is defined as the closest selection for an avoidance velocity, $V_{avo}^{\min}$, as expressed in equation (20).

$$S_{VO_P} = \frac{1}{2}\left|\sum_{t=0}^{n-1}(x_{vo}(t)y_{vo}(t+1) - x_{vo}(t+1)y_{vo}(t))\right| \tag{19}$$

$$V_{avo}^{\min} = \left\{V_{avo}(t)|t = \arg\min\sqrt{(x_{vo}(t) - V_o)^2 + (y_{vo}(t))^2}\right\} \tag{20}$$

where,

$$t = \left\{0, \frac{2\pi}{n}, \frac{4\pi}{n}, \ldots, \frac{2t\pi}{n}, 2\pi\right\} \tag{21}$$

B. Diverging Zone on an Avoidance Plane

Similar in the direct three dimensional VO method, the diverging zone DIV on an avoidance plane can be defined by moving the set of VO_P along the V_i, as shown in figure 10. It can be observed that the edges of the zone are the tangential lines of the VO_P from the origin, or A_o current position.

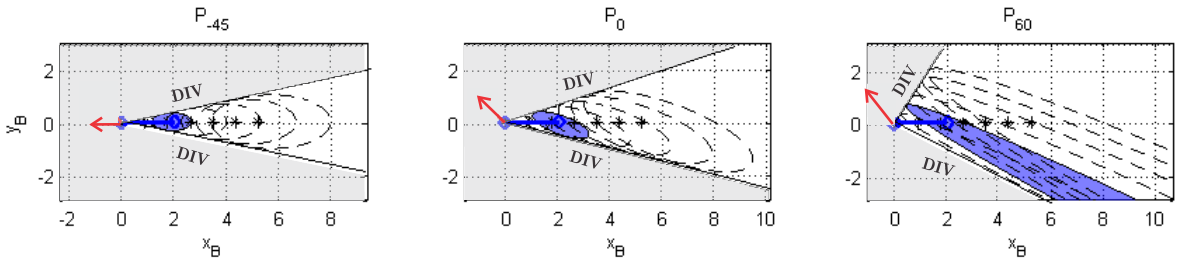

Figure 10. Diverging zone set, DIV, in three different avoidance-planes.

Using the VO_P as a polygon, those tangential lines are the two lines that pass through the origin and a vertex on the set that have the maximum or minimum value of gradient. The inclusion of V_o in the DIV_P set thus can be determined by checking if for each vertex, the criteria in equation (22) are fulfilled.

$$\forall t : \frac{y_{vo}(t)}{x_{vo}(t)} > 0 \quad \vee \quad \forall t : \frac{y_{vo}(t)}{x_{vo}(t)} < 0 \tag{22}$$

The diverging zone became more dominant in three dimensional cases. This means that restore-mode is easier to experience, especially with a high value of turning rate. Based on equation (22), for each avoidance plane, VO_P and DIV_P will always have two specific point of intersection, denoted as l_{vd}, which is also the two points that determined the DIV_P edges. This is true except for the degenerate cases.

C. Reachable Velocity Set on an Avoidance Plane

The RV can be defined in each avoidance plane as an area, which will simply revert back to its two dimensional fan-shaped area. Figure 11 shows the cross-sectional area of RV on two examples of avoidance planes, P_0, and P_{-90}, which corresponds to the ownship's XY, or longitudinal, and XZ, or lateral, -planes, respectively. Again, this is for the case shown in Figure 8.

RV definition neglects the effect of gravity, and therefore the RV on P_{90} is symmetrical, unlike the real longitudinal flight envelope of an aircraft, as shown in Ref.7. If the own-ship only considers these two planes, then the best avoidance for the case is either to turn right, or to decent, as they have the closest escape route from the VO. However, if the gravity effect is included, the easiest way to make avoidance is probably to descent, or to turn right on the P_{-90}. If A_o also considers how to escape to the DIV zone as soon as possible, the avoidance might be different. In this case, the own-ship needs to change its velocity directly to one of the l_{vd} points. With this in consideration, the opposite maneuvers to turn left or climb, are the better solution. These maneuvers make sense, since they go in the opposite direction of the obstacle.

Figure 11-a and -b also show the complete form of the VO sets on an example of avoidance-planes. The figure shows the entire feature of the selected avoidance-planes, including the representation of the main

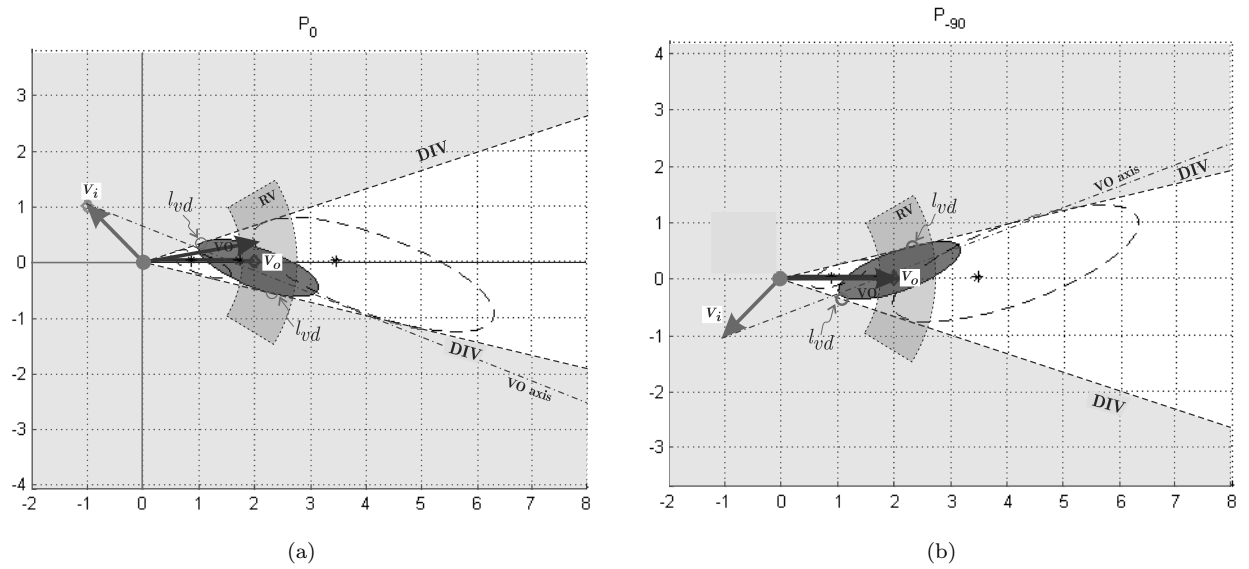

(a) (b)

Figure 11. Complete form of two example of the Avoidance Plane, for encounter case shown in Figure 8. (a) the P_0, represent the XY or longitudinal- plane, and (b) P_{-90}, which corresponds to A_os XZ, or lateral-planes of A_o body axis

sets, VO, DIV and RV, along with the VO cone axis of symmetry, and the intersection point of VO-DIV set, l_{vd}. The use of these features needs to be elaborated further, especially to determine its dynamics with the progression of the encounter.

V. Implementation

To evaluate the method presented in this paper, a computer simulation program has been developed. The simulated vehicles are assumed to exchange flight-data among each other, which includes the position, heading, and speed. The exchanges are assumed to be perfect without any losses or delays. The propagation of the avoidance maneuver in the simulation is shown using time-capture frames. Each vehicle involved is depicted as a point mass in the 3-dimensional space, set to have 5 meters/second of speed. The protected-zone of all dynamic (non-maneuvering) obstacles are depicted as spheres with radius of 10 meters. The own-ship starts its avoidance from $d_{avo} = 40$ m, with a constant turning-rate magnitude of 15 degrees/second. A special control algorithm is given to the own-ship in order to point back to a far original goal (500 meter away), after the obstacle is cleared.

A. Simulation 1: Two Vehicles Converging

This is the simulation of the case used in the explanation of the three dimensional Velocity Obstacle, shown in Figure 8. Here, A_o successfully avoids the protective zone S_{pz} of the obstacle using tree choice of avoidance plane, P_0, P_{45}, and P_{-90}.

The own-ship in the simulation is able to avoid the obstacle, with the nearest distance of 10 meters, exactly at the Protected Zone sphere surface, as also shown in Figure 14. The three Avoidance planes are demonstrated able to avoid collision with the intruder. Which plane is the optimal avoidance, however, requires further extraction from the simulation result.

It should be note that work of avoidance using the Velocity Obstacle method ends on the highest point of each avoidance, where the course is considered as clear. The pointing back to the original goal (restore) is the work of a control system separately from the 3-dimensional Velocity Obstacle.

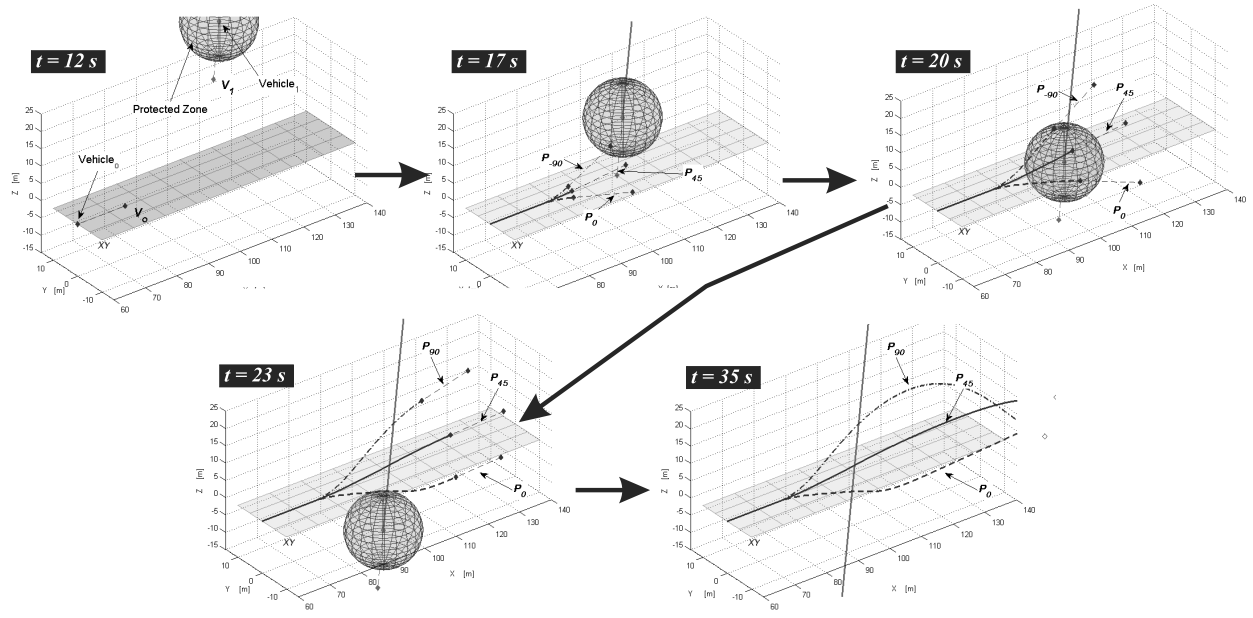

Figure 12. Simulation-1: The case shown in Figure 8. Three choice of avoidance plane is given, P_0, P_{45}, and P_{-90}

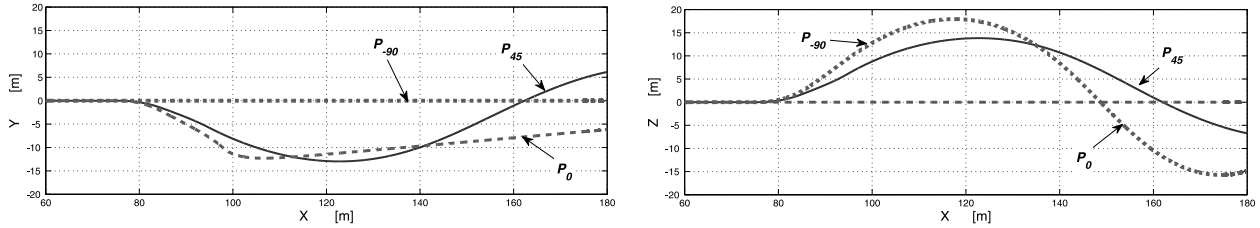

(a) (b)

Figure 13. Simulation-1: (a) Top-view and (d) Side View of the own-ship flight-path in its avoidance, using three choice of avoidance plane, P_0, P_{45}, and P_{-90}

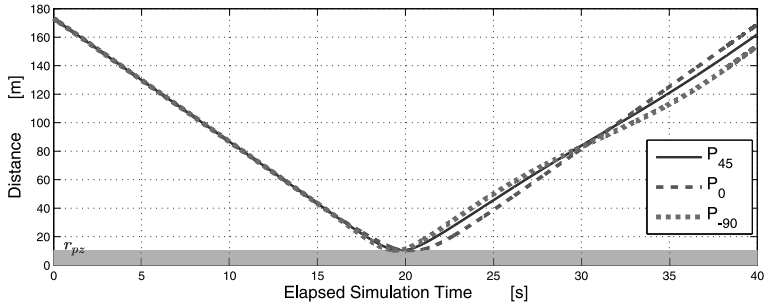

Figure 14. Simulation-1: Distance through the simulation time, with three choice of avoidance plane P_0, P_{45}, and P_{-90}

B. Simulation 2: Multiple Conflicts

Figure 15 shows the simulation of the case of multiple 3-dimensional conflicts, avoided by the ownship using three different avoidance plane. Here, three obstacle, V_1, V_2 and V_3 are set to collide with the own-ship along its path. The own-ship avoid by turning on an avoidance plane that produce the smallest conic-sections, i.e.

P_{45}, P_0, and P_{-90}, respectively. The avoidance is conducted based on the distance priority,

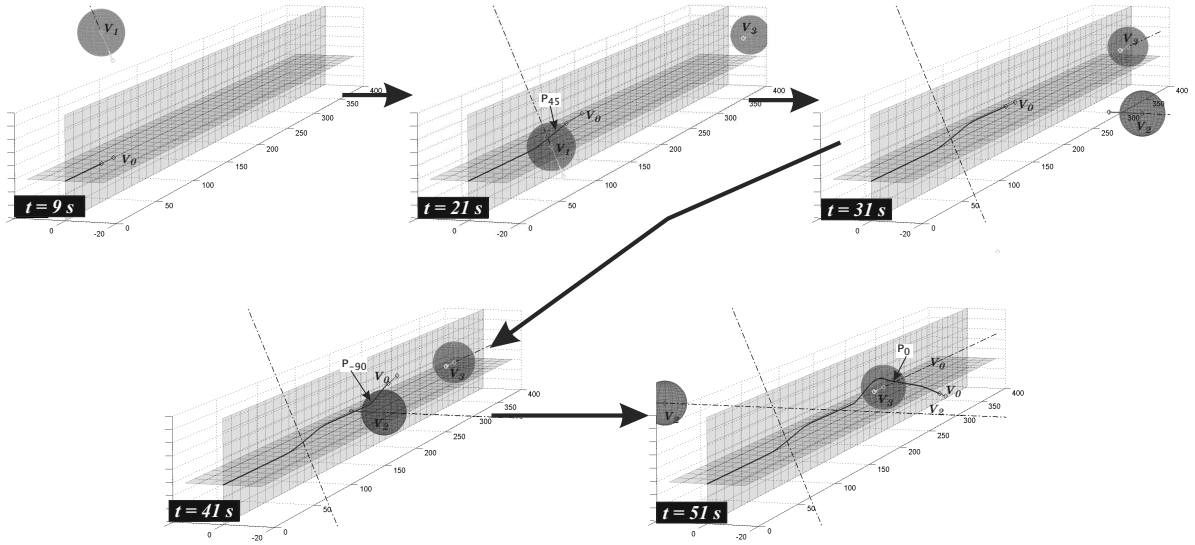

Figure 15. Simulation-2: Multiple 3-dimensional conflicts, avoided by the ownship using three different avoidance plane, i.e. the smallest VO conic section.

VI. Conclusion

This paper focuses on the assessment of the Velocity Obstacle Method to autonomously resolve three-dimensional conflicts for Unmanned Aerial Vehicles (UAVs). A novel technique to represent the three-dimensional conflict in various avoidance-planes is introduced to help the avoidance decision making.

The use of avoidance-planes reveals many interactions between the conflict and the avoidance maneuver in three-dimensions. Choosing an avoidance plane on P_{xy} or P_{xz} will result in a pure turn or climb/descent, respectively. The risk value for each avoidance-plane can be defined by the area of the VO conic-section in each avoidance-plane. An avoidance with highest risk is experienced whenever the vehicle chooses an avoidance plane on which lies the obstacle velocity vector V_i. The least-risk avoidance, on the other hand, occurs on the avoidance-plane that is perpendicular from the previous. The risk value, however, may not necessary be related to the avoidance-plane with the shortest path.

Simulations are conducted to assess the performance of the algorithm in a single or multiple conflict. Further analysis need to be conducted to determined the effectiveness and efficiency of the maneuver, related to the aim of deconflict maneuver.

The large domination of diverging areas in three-dimensional cases suggest that it is easier for a vehicle to avoid conflict, compared to the two dimensional case. On every avoidance-plane exists two points of VO - DIV intersection, which represent the fastest escape route from VO. However, oscillation is expected to occur. The technique needs to be elaborated further, especially for dynamic changes of the avoidance-plane. The reciprocating cases are left for the future work as well.

References

[1]DeGarmo, M. T. and Nelson, G. M., "Prospective unmanned aerial vehicle operations in the future national airspace system," *AIAA 4th Aviation Technology, Integration, and Operations Forum, ATIO*, AIAA, 2004, pp. 172–179, AIAA 2004-6243, doi:10.2514/6.2004-6243.

[2]Jenie, Y. I., van Kampen, E., de Visser, C. C., and Chu, Q. P., "Selective Velocity Obstacle Method for Cooperative Autonomous Collision Avoidance System for UAVs," *AIAA Guidance, Navigation, and Control Conference 2013*, AIAA, Boston, MA, 2013, AIAA 2013-4627, doi:10.2514/6.2013-4627.

[3]Hoekstra, J. M., Ruigrok, R. C. J., and van Gent, R. N. H. W., "Free Flight in a Crowded Airspace ?" *3rd USA/Europe Air Traffic Management R & D Seminar - Proceedings*, EUROCONTROL, Napoli, 2000.

[4]Hoekstra, J. M., "Designing for Safety: the Free Flight Air Traffic Management concept," 2001.

[5]Barfield, F., "Autonomous collision avoidance. The technical requirements," *National Aerospace and Electronics Conference (NAECON)*, 2000, pp. 808–813, doi:10.1109/NAECON.2000.894998.

[6]Ellerbroek, J., Visser, M., van Dam, S. B. J., Mulder, M., and van Paassen, M. M., "Design of an Airborne Three-Dimensional Separation Assistance Display," *IEEE Transactions on Systems, Man, and Cybernetics, part A: Systems and Humans*, Vol. 41, No. 6, 2011, pp. 863–875, doi:10.1109/TSMCA.2010.2093890.

[7]Ellerbroek, J., Brantegem, K. C. R., van Paassen, M. M., and Mulder, M., "Design of a Co-Planar Airborne Separation Display," *IEEE Transactions on Human-Machine Systems*, Vol. 43, No. 3, 2013, pp. 277–289, doi:10.1109/TSMC.2013.2242888.

[8]Fiorini, P. and Shiller, Z., "Motion Planning in Dynamic Environments Using Velocity Obstacles," *The International Journal of Robotics Research*, Vol. 17, No. 7, 1998, pp. 760–772, doi:10.1177/027836499801700706.

[9]Kluge, B. and Prassler, E., "Recursive Probabilistic Velocity Obstacles for Reflective Navigation," *Field and Service Robotics*, edited by S. Yuta, H. Asama, E. Prassler, T. Tsubouchi, and S. Thrun, Vol. 24 of *Springer Tracts in Advanced Robotics*, Springer Berlin Heidelberg, 2006, pp. 71–79, doi:10.1007/10991459_8.

[10]van der Berg, J., Lin, M., and Manocha, D., "Reciprocal Velocity Obstacles for Real-Time Multi-Agent Navigation," *International Conference on Robotics and Automation*, IEEE, Pasadena, CA, USA, 2008, doi:10.1109/ROBOT.2008.4543489.

[11]van Dam, S. B. J., Mulder, M., and Van Paassen, M., "Ecological Interface Design of a Tactical Airborne Separation Assistance Tool," *Systems, Man and Cybernetics, Part A: Systems and Humans, IEEE Transactions on*, Vol. 38, No. 6, Nov 2008, pp. 1221–1233, doi:10.1109/TSMCA.2008.2001069.

[12]Heylen, F. M., van, S. B. J., Mulder, M., and van Paassen, M. M., "Design and Evaluation of a Vertical Separation Assistance Display," *AIAA Guidance, Navigation, and Control Conference and Exhibit*, Honolulu (HI), 2008, AIAA 2008-6969, doi:10.2514/6.2008-6969.

[13]Snape, J., van den Berg, J., Guy, S., and Manocha, D., "The Hybrid Reciprocal Velocity Obstacle," *Robotics, IEEE Transactions on*, Vol. 27, No. 4, Aug 2011, pp. 696–706, doi:10.1109/TRO.2011.2120810.

[14]Jenie, Y. I., van Kampen, E.-J., and Remes, B., "Cooperative Autonomous Collision Avoidance System for Unmanned Aerial Vehicle," *Advances in Aerospace Guidance, Navigation and Control*, edited by Q. Chu, B. Mulder, D. Choukroun, E.-J. Kampen, C. Visser, and G. Looye, Springer Berlin Heidelberg, 2013, pp. 387–405, doi:10.1007/978-3-642-38253-6_24.

[15]Kluge, B., "Recursive Probabilistic Velocity Obstacles for Reflective Navigation," *Proc. of 1st Int. Workshop on Advances in Service Robots.*, 2003.

[16]Hurley, R. D., Lind, R., and Kehoe, J. J., "A Torus Based Three Dimensional Motion Planning Model for Very Maneuverable Micro Air Vehicles," *AIAA Guidance, Navigation, and Control Conference 2013*, AIAA, Boston, MA, 2013, AIAA 2013-4938, doi:10.2514/6.2013-4938.